
A NESTED KRYLOV METHOD USING HALF-PRECISION ARITHMETIC

A PREPRINT

 **Kengo Suzuki**

Academic Center for Computing and Media Studies,
Kyoto University,
Kyoto, Japan
suzuki@i.kyoto-u.ac.jp

Takeshi Iwashita

Academic Center for Computing and Media Studies,
Kyoto University,
Kyoto, Japan
iwashita@i.kyoto-u.ac.jp

June 7, 2025

ABSTRACT

Low-precision computing is essential for efficiently utilizing memory bandwidth and computing cores. While many mixed-precision algorithms have been developed for iterative sparse linear solvers, effectively leveraging half-precision (fp16) arithmetic remains challenging. This study introduces a novel nested Krylov approach that integrates the FGMRES and Richardson methods in a deeply nested structure, progressively reducing precision from double-precision to fp16 toward the innermost solver. To avoid meaningless computations beyond precision limits, the low-precision inner solvers perform only a few iterations per invocation, while the nested structure ensures their frequent execution. Numerical experiments show that incorporating fp16 into the approach directly enhances solver performance without compromising convergence, achieving speedups of up to $1.65 \times$ and $2.42 \times$ over double-precision and double-single mixed-precision implementations, respectively. Furthermore, the proposed method outperforms conventional mixed-precision Krylov solvers, CG, BiCGStab, and restarted FGMRES, by factors of up to 2.47, 2.74, and 69.10, respectively.

Keywords Sparse linear solvers · Mixed-precision algorithms · Half-precision · Nested Krylov methods

1 Introduction

We explore solving sparse linear systems, $\mathbf{A}\mathbf{x} = \mathbf{b}$, where $\mathbf{A} \in \mathbb{R}^{n \times n}$ and $\mathbf{b}, \mathbf{x} \in \mathbb{R}^n$, using iterative methods with low-precision arithmetic and data types. Because most computing kernels in sparse iterative methods are memory-bounded, reducing data movement directly improves performance. Using low-precision arithmetic is also motivated by a recent trend in hardware development where computing units are simplified to increase parallelism. Hence, significant efforts have been made to realize practical sparse linear solvers in low-precision, with many proposals and evaluations (Abdelfattah et al., 2021; Higham and Mary, 2022). Among these, mixed-precision algorithms, particularly Generalized Minimal Residual (GMRES) algorithms, have received considerable attention (Turner and Walker, 1992; Anzt et al., 2011; Lindquist et al., 2021; Zhao et al., 2022; Carson et al., 2022), leading to a proposal of a mixed-precision benchmark, HPGMP (Yamazaki et al., 2022), as a successor to the HPCG benchmark. While their practicality has steadily improved, there is room for improvement in using half-precision (fp16). In particular, despite its prevalence in direct methods, fp16 remains relatively unexplored in sparse iterative methods. Furthermore, existing research mainly focuses on the precision of preconditioners (Carson and Khan, 2023; Scott and Tůma, 2024), with very few studies investigating the use of fp16 in the main part of sparse iterative methods. This rareness is primarily due to the significant degradation in the convergence speed by fp16 even in algorithms where single-precision (fp32) works well (Aliaga et al., 2023).

To leverage fp16 arithmetic effectively, we introduce a novel nested Krylov-based approach that integrates flexible GMRES (FGMRES) (Saad, 2003) and Richardson (Richardson, 1911) methods. As shown in previous work (e.g., Reference (Yamazaki et al., 2022)), low-precision GMRES can partially reduce residuals, even when using a unified

precision (e.g., fp32 or fp16). Our approach exploits this property by progressively reducing both precision and the number of iterations toward the innermost solver. Low-precision inner solvers perform only a few iterations per invocation to prevent exceeding precision limits, while the nested structure increases the proportion of low-precision computations. We also provide an adaptive technique for updating the weight in the fp16 Richardson part, which is located in the innermost and affects solver performance significantly. The adaptive technique enhances the stability of our method. We perform numerical experiments on both CPU and GPU nodes and show that our method outperforms standard Krylov methods, including restarted FGMRES, Conjugate Gradient (CG) and Bi-CG Stabilized (BiCGStab) (Saad, 2003).

The rest of this paper is structured as follows. In Section 2, we review previous mixed-precision algorithms and the nested Krylov framework. Here, we also clarify the difference between this study and previous studies. In Section 3, we introduce a notation and terminology for nested Krylov. In Section 4, we explain the proposed approach. First, we evaluate it in comparison with the restarted FGMRES, CG, and BiCGStab methods in Section 5. Next, we give more detailed analyses of its parameter setting in Section 6. Finally, we conclude the study in Section 7.

2 Related Work and Contributions

Mixed-precision algorithms are widely used across various applications in numerical linear algebra (Abdelfattah et al., 2021; Higham and Mary, 2022), with mixed-precision solvers developed for both dense and sparse linear systems. For solvers that incorporate direct methods like LU (Cholesky) factorization, numerous techniques exploit fp32 and fp16 (Carson and Higham, 2017; Haidar et al., 2018; Abdelfattah et al., 2020; Amestoy et al., 2024).

In sparse iterative solvers, which we focus on, low-precision arithmetic is typically integrated in two ways: within parts of the solver or by nesting a low-precision solver as a preconditioner within an outer high-precision solver. The former approach often involves reducing the precision of preconditioners. Many techniques have been proposed to utilize fp32 and fp16 in preconditioners, including incomplete Cholesky, approximate inverse, and multigrid preconditioners (Zong et al., 2024; Scott and Tůma, 2024; Carson and Khan, 2023). Another strategy is to reduce the precision of the sparse matrix-vector multiplication (SpMV) kernel, a core component of sparse iterative solvers. Several studies have shown the viability of low-precision SpMV in Krylov solvers (Simoncini and Szyld, 2003; Graillat et al., 2024). Additionally, some methods reduce the precision of specific variables in the solver, such as the Arnoldi basis in GMRES (Aliaga et al., 2023; Grützmacher et al., 2024), where 32-bit types can be effective, though fp16 offers less benefit.

The latter approach frequently employs iterative refinement, where a low-precision solver serves as a preconditioner for a high-precision Richardson solver. GMRES is commonly used because of its affinity with restarting included in iterative refinement. The effectiveness of using GMRES implemented using fp32 or 32-bit integers as the inner solver has been explored both numerically and analytically (Anzt et al., 2011; Loe et al., 2021; Zhao et al., 2022; Lindquist et al., 2021; Suzuki et al., 2024). Using other iterative methods, such as CG and BiCGStab, as the inner solver have also been investigated (Zhao et al., 2023; Higham and Pranesh, 2021). Furthermore, some studies uses more sophisticated solvers, such as double-precision (fp64) FGMRES and CG, as the outer solver instead of iterative refinement (Baboulin et al., 2009; Buttari et al., 2008).

Another important technique related to this study is nested Krylov, a framework that recursively uses one Krylov solver as a preconditioner for another Krylov solver. One of the most well-known instances of it would be the flexible inner-outer GMRES method (Saad, 1993), where a preconditioned GMRES method is used as a preconditioner of the FGMRES method. Besides, several other variations have been developed individually for specific purposes (Golub and Ye, 1999; Axelsson et al., 2004). The nested Krylov framework is discussed systematically in Reference (McInnes et al., 2014), particularly within the context of reducing communication overhead in distributed systems. Note that nested Krylov can, in principle, accept any iterative methods other than the Krylov method despite its name, as the Chebyshev iteration is used in Reference (McInnes et al., 2014).

2.1 Contributions

While these previous studies on mixed-precision algorithms have mainly focused on two-level nesting and using fp32, this study distinguishes itself by exploiting low-precision arithmetic in three- or higher-level nested structures and investigating the use of fp16. Consequently, the main contributions of this study are as follows:

- We propose a mixed-precision (fp64, fp32, and fp16) approach by integrating FGMRES and Richardson in the nested Krylov framework. In the approach, we gradually reduce the precision towards the innermost solver to achieve effective use of fp16.

- We adopt an fp16 Richardson solver in the innermost part and also propose a technique for controlling its weight adaptively.
- We show that our solver outperforms conventional mixed-precision solvers through numerical experiments on CPU and GPU nodes. Notably, our solver is superior to preconditioned CG even for several symmetric positive definite matrices.

3 Notation

For clarity, we express nested Krylov solvers using tuples. A pair $(\mathbf{S}^{(1)}, \mathbf{M})$ denotes a solver $\mathbf{S}^{(1)}$ preconditioned by \mathbf{M} . Similarly, if $\mathbf{S}^{(1)}$ is preconditioned by another nested solver $(\mathbf{S}^{(2)}, \mathbf{M})$, it is written as $(\mathbf{S}^{(1)}, (\mathbf{S}^{(2)}, \mathbf{M}))$. For simplicity, we also express it as $(\mathbf{S}^{(1)}, \mathbf{S}^{(2)}, \mathbf{M})$ following the standard notation for ordered tuples. This naturally extends to deeper levels of nesting, resulting in the general form $(\mathbf{S}^{(1)}, \mathbf{S}^{(2)}, \dots, \mathbf{S}^{(D)}, \mathbf{M})$, where D is the depth level of the nested solver. For readability, we introduce the following terminology. The solvers $\mathbf{S}^{(2)}$ through $\mathbf{S}^{(D)}$ are referred to as inner solvers, while $\mathbf{S}^{(1)}$ and $\mathbf{S}^{(D)}$ are called the outermost and innermost solvers, respectively. Moreover, $\mathbf{S}^{(d-1)}$ (for $d = 2, \dots, D$) is referred to as the parent solver of $\mathbf{S}^{(d)}$. The preconditioner \mathbf{M} is called the primary preconditioner because an inner solver $\mathbf{S}^{(d)}$ can also be regarded as a preconditioner of its parent solver. In this study, \mathbf{M} is assumed to be an algebraic preconditioner, such as an incomplete LU (ILU) preconditioner. Lastly, FGMRES and Richardson of m iterations are denoted as \mathbf{F}_m and \mathbf{R}_m , respectively.

4 Nested Krylov-Based Approach

Previous studies have shown that the performance of low-precision GMRES in the early iterations can be comparable to that of full-precision GMRES, even in the case of uniform-precision implementations (Yamazaki et al., 2022; Zhao et al., 2022). This suggests that low-precision arithmetic is effective when the number of iterations per invocation is limited. Building on this insight we propose a novel mixed-precision approach that utilizes fp16 arithmetic effectively. Our method employs a nested Krylov structure, integrating multiple FGMRES and Richardson solvers while gradually reducing precision from fp64 to fp16 and decreasing the number of iterations towards the innermost solver. Since each inner solver runs only a few iterations per invocation, the negative effect of using low precision on convergence is expected to be small. However, because these inner solvers are invoked at every iteration of their parent solvers, low-precision arithmetic is performed frequently. As a result, our approach can achieve a high frequency of fp16 computations without deteriorating convergence.

4.1 Our Strategy for Nesting

In our approach, we have various possible settings for the nesting depth and the number of iterations of each part. To find effective configurations, we consider convergence speed and the amount of memory accesses per iteration, both of which are key factors in solver performance. First, we make the following assumptions with respect to the convergence speed, whose validity is examined in Section 6:

- when m is relatively large, for \bar{m} and $\bar{\bar{m}}$ such that $m = \bar{m}\bar{\bar{m}}$, we can approximate $(\mathbf{F}_m, \mathbf{M})$ with a nested solver $(\mathbf{F}_{\bar{m}}, (\mathbf{F}_{\bar{\bar{m}}}, \mathbf{M}))$ without reducing the convergence speed.
- when m is small (e.g., $m < 5$), we can replace $(\mathbf{F}_m, \mathbf{M})$ with $(\mathbf{R}_m, \mathbf{M})$ without compromising the convergence speed.

We expect these assumptions to hold when the primary preconditioner \mathbf{M} is sufficiently effective.

Under these assumptions, we focus on the amount of memory accesses, the other key factor to achieving high performance. We therefore introduce a rough model of the amount of memory accesses per n of $(\mathbf{F}_m, \mathbf{M})$, $O_{(\mathbf{F}_m, \mathbf{M})}$, and that of $(\mathbf{R}_m, \mathbf{M})$, $O_{(\mathbf{R}_m, \mathbf{M})}$, as

$$\begin{aligned} O_{(\mathbf{F}_m, \mathbf{M})} &:= c_A m + c_M m + \frac{5}{2} m^2, \\ O_{(\mathbf{R}_m, \mathbf{M})} &:= c_A(m-1) + c_M m + 4(m-1), \end{aligned} \tag{1}$$

where c_A and c_M are constants associated with the number of nonzeros per row of the coefficient matrix \mathbf{A} and preconditioner \mathbf{M} , respectively. Terms $c_A(m-1)$ and $4(m-1)$ in $O_{(\mathbf{R}_m, \mathbf{M})}$ reflect that we assume the initial guess to be a zero vector. Note that these models are intended to provide a rough guideline, and we here do not consider exact models, which must include complicated factors such as data types, cache utilization, and implementation details.

Then, we consider the memory access model of two-level nested FGMRES $(\mathbf{F}_{\bar{m}}, \mathbf{F}_{\bar{m}}, \mathbf{M})$, $O_{(\mathbf{F}_{\bar{m}}, \mathbf{F}_{\bar{m}}, \mathbf{M})}$, while assuming $m = \bar{m}\bar{m}$ to fix the number of calls to the primary preconditioner \mathbf{M} :

$$\begin{aligned} O_{(\mathbf{F}_{\bar{m}}, \mathbf{F}_{\bar{m}}, \mathbf{M})} &:= c_A \bar{m} + O_{(\mathbf{F}_{\bar{m}}, \mathbf{M})} \bar{m} + \frac{5}{2} \bar{m}^2 \\ &= O_{(\mathbf{F}_m, \mathbf{M})} + c_A \bar{m} + \frac{5}{2} \bar{m}^2 \bar{m} + \frac{5}{2} \bar{m}^2 - \frac{5}{2} m^2. \end{aligned} \quad (2)$$

This equation provides an estimation of the overhead and benefits of dividing reference FGMRES into two-level nested FGMRES. When m is relatively large, nesting offers a significant advantage due to the reduced cost of the Arnoldi process. In other words, in such cases, splitting FGMRES has the benefit of both reducing memory accesses and improving the usability of low precision by reducing the number of iterations per call. For example, assuming $c_A = 45$ (30 nonzeros per row, with fp64 for values and 32-bit integers for indices) and $m = 64$, the inequity $O_{(\mathbf{F}_{\bar{m}}, \mathbf{F}_{\bar{m}}, \mathbf{M})} < O_{(\mathbf{F}_m, \mathbf{M})}$ holds for most possible values of \bar{m} , and $\bar{m} = 10$ results in the least amount, though 10 is not a divisor of 64. On the other hand, for small values of m , Equation (2) also indicates that nesting rather increases memory accesses. This would be a problem when m is still too large to implement the inner solver in lower-precision such as fp16. However, if we replace the inner FGMRES with Richardson, the amount becomes

$$\begin{aligned} O_{(\mathbf{F}_{\bar{m}}, \mathbf{R}_{\bar{m}}, \mathbf{M})} &:= c_A \bar{m} + O_{(\mathbf{R}_{\bar{m}}, \mathbf{M})} \bar{m} + \frac{5}{2} \bar{m}^2 \\ &= O_{(\mathbf{F}_m, \mathbf{M})} + 4(\bar{m} - 1)\bar{m} + \frac{5}{2} \bar{m}^2 - \frac{5}{2} m^2. \end{aligned} \quad (3)$$

This leads to fewer memory accesses for all possible values of \bar{m} when $m \geq 3$. Thus, we will achieve higher performance by replacing the inner FGMRES with Richardson as long as Assumption (ii) remains valid.

In summary, we split a baseline FGMRES solver into a nested solver, where inner solvers perform a few iterations for the use of low-precision arithmetic. To achieve this, we take the following strategy. Building on Assumption (i), we recursively divide an inner FGMRES solver into a nested FGMRES solver while considering reducing memory accesses based on Equation (2). Even when Equation (2) indicates that nesting increases memory accesses, replacing FGMRES with Richardson can reduce memory accesses as shown in Equation (3). Therefore, while Assumption (ii) holds, we may consider using Richardson instead of inner FGMRES.

4.2 Proposed Solver: F3R

Following the strategy outlined above, we develop an instance of our nested Krylov-based approach, named F3R. It consists of three FGMRES solvers and an innermost Richardson solver, defined as $(\mathbf{F}_{m_1}, \mathbf{F}_{m_2}, \mathbf{F}_{m_3}, \mathbf{R}_{m_4}, \mathbf{M})$ in the tuple notation, with default parameters $(m_1, m_2, m_3, m_4) = (100, 8, 4, 2)$. The development process of F3R is as follows.

First, we select $(\mathbf{F}_{64}, \mathbf{M})$ as a reference. Subsequently, we approximate it with $(\mathbf{F}_{m_2}, \mathbf{F}_{m'_3}, \mathbf{M})$. Given the considerations of the amount of memory accesses in Equation (2), we choose $m_2 = 8$, a value considered near-optimal among the divisors of 64; then, $m'_3 = 8 (= 64/m_2)$. Presuming that $m'_3 = 8$ is still too large for implementing FGMRES in fp16, we attempt to further divide the inner solver $(\mathbf{F}_{m'_3}, \mathbf{M})$ into $(\mathbf{F}_{m_3}, \mathbf{F}_{m_4}, \mathbf{M})$. However, this will increase memory accesses, according to Equation (2). Thus, we replace \mathbf{F}_{m_4} with \mathbf{R}_{m_4} ; that is, we divide $(\mathbf{F}_{m'_3}, \mathbf{M})$ into $(\mathbf{F}_{m_3}, \mathbf{R}_{m_4}, \mathbf{M})$. While there are several possible choices for m_4 , we opt $m_4 = 2$ considering Assumption (ii). Finally, we wrap $(\mathbf{F}_{m_2}, \mathbf{F}_{m_3}, \mathbf{R}_{m_4}, \mathbf{M})$ with \mathbf{F}_{m_1} , rather than restarting (or iterative refinement), for better performance, and we set $m_1 = 100$ empirically.

Convergence is checked only in the outermost \mathbf{F}_{m_1} . In practice, if convergence is not reached within 100 outermost iterations, we execute the entire solver $(\mathbf{F}_{m_1}, \mathbf{F}_{m_2}, \mathbf{F}_{m_3}, \mathbf{R}_{m_4}, \mathbf{M})$ again in the manner of the restarting technique.

We implement F3R in mixed precision as specified in Table 1. Starting from fp64 for the outermost FGMRES \mathbf{F}_{m_1} , we progressively reduce precision towards the innermost fp16 Richardson $(\mathbf{R}_{m_4}, \mathbf{M})$. The Richardson method has a straightforward recurrence and avoids reduction kernels, such as the norm kernel, which are susceptible to numerical errors. Moreover, we set m_4 to 2, a small value. Thus, using fp16 would not significantly affect computational accuracy. The two inner FGMRES solvers, \mathbf{F}_{m_2} and \mathbf{F}_{m_3} , are also implemented in low precision. These solvers include reduction kernels, so we store their variables in fp32. Specifically, as we employ classical Gram-Schmidt and Givens rotation for the Arnoldi process and the QR factorization, all associated computations are performed only with vectors and scalars stored in fp32. While \mathbf{F}_{m_2} employs an fp32 SpMV kernel, \mathbf{F}_{m_3} stores \mathbf{A} in fp16. This choice is based on the fact that \mathbf{F}_{m_3} serves as a preconditioner for \mathbf{F}_{m_2} , where higher precision would not be necessitated. Finally, \mathbf{F}_{m_1} is implemented in fp64 to provide an accurate approximate solution. Throughout the implementation, higher-precision instructions are used when the inputs differ in precision. For example, \mathbf{F}_{m_3} performs SpMV in fp32 because \mathbf{A} is stored in fp16 while the input Arnoldi basis is in fp32.

Table 1: Details of the proposed method F3R.

Solver	Default	Precision		
		\mathbf{A}	Vectors	\mathbf{M}
\mathbf{F}_{m_1}	$m_1 = 100$	fp64	fp64	-
\mathbf{F}_{m_2}	$m_2 = 8$	fp32	fp32	-
\mathbf{F}_{m_3}	$m_3 = 4$	fp16	fp32	-
\mathbf{R}_{m_4}	$m_4 = 2$	fp16	fp16	fp16

Algorithm 1: Richardson with adaptive weight-updating

Data: Linear system $\mathbf{A}\mathbf{z} = \mathbf{v}$, preconditioner \mathbf{M} , weights $\omega_1, \dots, \omega_{m_4}$, and call count of Algorithm 1 c_{ntr} .
Result: Approximate solution \mathbf{z}_{m_4} , weights $\omega_1, \dots, \omega_{m_4}$, and call count of this algorithm c_{ntr} .
/* $\omega_1, \dots, \omega_{m_4}$ and c_{ntr} are global variables and retain their values across function calls. */

```

1 if  $c_{ntr} = 1$  (the first call) then
2   | Initialize  $\omega_1 = \dots = \omega_{m_4} = 1$ .
3 end
4 Assume  $\mathbf{z}_0 = \mathbf{0}$ .
5 for  $k := 1, \dots, m_4$  do
6   |  $\mathbf{r}_{k-1} := \mathbf{v} - \mathbf{A}\mathbf{z}_{k-1}$                                 //  $\mathbf{r}_0 = \mathbf{v}$  without calculation.
7   | if  $c_{ntr} \equiv 0 \pmod{c}$  then
8     |   |  $\omega'_k = (\mathbf{r}_{k-1}, \mathbf{A}\mathbf{M}\mathbf{r}_{k-1}) / (\mathbf{A}\mathbf{M}\mathbf{r}_{k-1}, \mathbf{A}\mathbf{M}\mathbf{r}_{k-1})$ 
9     |   |  $\mathbf{z}_k = \mathbf{z}_{k-1} + \omega'_k \mathbf{M}\mathbf{r}_{k-1}$ 
10    |   |  $\omega_k := (l\omega_k + \omega'_k) / (l + 1)$  for  $l := c_{ntr} / c$ 
11   | else
12     |   |  $\mathbf{z}_k = \mathbf{z}_{k-1} + \omega_k \mathbf{M}\mathbf{r}_{k-1}$ 
13   | end
14 end
15 Increment  $c_{ntr} := c_{ntr} + 1$ 

```

One may assume that the setting of $m_4 = 2$ for the innermost fp16 Richardson solver is too small. However, we emphasize that the innermost solver performs $m_2 m_3 m_4$ iterations per outermost iteration in total, achieving a high frequency of fp16 computations.

4.3 Adaptive Weight Updating

Finally, we consider the weight in the innermost Richardson part, $(\mathbf{R}_{m_4}, \mathbf{M})$, of F3R, which is crucial for holding Assumption (ii). This Richardson part receives a vector \mathbf{v} and searches an approximate solution of a linear system $\mathbf{A}\mathbf{z} = \mathbf{v}$ as a preconditioning step of its parent solver. Specifically, at the k -th ($k = 1, \dots, m_4$) iteration, it computes an approximate solution \mathbf{z}_k as

$$\mathbf{z}_k = \mathbf{z}_{k-1} + \omega \mathbf{M}(\mathbf{v} - \mathbf{A}\mathbf{z}_{k-1}), \quad (4)$$

where ω is a scalar value, weight. Since Richardson is a stationary iterative method, its convergence speed depends on the spectral radius of $\mathbf{I} - \omega \mathbf{M} \mathbf{A}$. Therefore, to satisfy Assumption (ii), it is important to consider not only the choice of the primary preconditioner \mathbf{M} but also the quality of the weight ω . Although the optimal weight depends on the eigenvalues of $\mathbf{M} \mathbf{A}$ and is impractical to compute, a locally optimal value can be easily determined at each iteration. The k -th residual \mathbf{r}_k in Richardson is given as

$$\mathbf{r}_k = \mathbf{r}_{k-1} - \omega \mathbf{A}\mathbf{M}\mathbf{r}_{k-1}.$$

Thus, the weight ω'_k that minimizes the 2-norm of \mathbf{r}_k is found as

$$\omega'_k = \frac{(\mathbf{r}_{k-1}, \mathbf{A}\mathbf{M}\mathbf{r}_{k-1})}{(\mathbf{A}\mathbf{M}\mathbf{r}_{k-1}, \mathbf{A}\mathbf{M}\mathbf{r}_{k-1})}.$$

If ω'_k is computed at every iteration, it is equivalent to GMRES(1), and Assumption (ii) may have some validity. However, this approach undermines the advantage of Richardson, as it incurs additional SpMV and reduction computations.

Conversely, using a single ω'_k persistently throughout the whole iteration or for the entire solution process may also be ineffective; there is no guarantee that ω'_k remains optimal in subsequent iterations or for different linear systems at other preconditioning steps of the parent solver.

Therefore, we propose a technique to estimate an appropriate value ω_k for each iteration by updating it over successive invocations of the Richardson solver. While the optimal value of ω is unique, we use k different weights ω_k for flexibility. Specifically, we initialize ω_k as 1 and update it by computing ω'_k every c calls to the Richardson solver, using the cumulative average of all previously computed weights:

$$\omega_k := \frac{l\omega_k + \omega'_k}{l + 1}, \quad (5)$$

where l is the update count, defined as the number of invocations of the Richardson solver divided by c . Importantly, this adaptive technique updates ω_k across all invocations of the Richardson part because the optimal weight does not depend on the right-hand side of a given linear system. Consequently, the technique is expected to prevent ω_k from becoming overly localized, while keeping the additional computational cost low. Algorithm 1 outlines the complete process of the Richardson part with this adaptive weight-updating technique. It is noteworthy that when updating ω_k on lines 7–11, ω'_k is used as the weight, rather than ω_k , because it minimizes the residual at that step. The effectiveness of this technique is evaluated through numerical experiments in Section 6. It should be mentioned that the process for computing ω'_k is implemented in fp32, although other parts of the innermost Richardson is implemented in fp16 as explained in Section 4.2.

Our nested Krylov approach, in principle, accepts Richardson at multiple levels. Note that in such cases, the weight ω_k should be handled separately at each level. This is because the optimal value of a Richardson part depends on its preconditioner (inner solver), not the primary preconditioner, which differs from level to level.

5 Experimental Results

In this section, we evaluate the effect of reducing precision on the performance of F3R and compare F3R with three conventional preconditioned Krylov methods, restarted FGMRES of a restart cycle of 64 (FGMRES(64)), CG, and BiCGStab, both on CPU and GPU nodes. In addition to the setting outlined in Table 1, we implemented F3R in only fp64 or fp64-fp32 mixed precision; the latter use fp32 for all the inner solvers. To distinguish them, we refer to the implementation that uses three precisions, fp64, fp32, and fp16, shown in Table 1, as fp16-F3R, while we label the additional two as fp64-F3R and fp32-F3R, respectively. Leaving the detailed examination of the parameters, m_1 , m_2 , m_3 , m_4 , and c , to Section 6, this section focuses primarily on results with the default setting ($m_1 = 100$, $m_2 = 8$, $m_3 = 4$, $m_4 = 2$, and $c = 64$). We also present results for fp16-F3R configured for optimal performance, which is referred to as fp16-F3R-best. For each of the other Krylov methods, FGMRES(64), CG, and BiCGStab, we developed three fp64-based solvers, varying the precision of the preconditioner storage between fp64, fp32, and fp16. When reducing the precision of the preconditioner, we first construct it in fp64 and then cast its values to fp32 or fp16. Similar to F3R, these are prefixed by fp64, fp32, and fp16: e.g., fp16-CG for fp64 CG with an fp16 preconditioner. All the solvers used 32-bit integers for column indices and index pointer arrays in storing matrices.

We tested several larger-size matrices from the SuiteSparse Matrix Collection (Davis and Hu, 2011), the HPGM benchmark (Dongarra et al., 2016), and the HPGMP benchmark (Yamazaki et al., 2022), shown in Table 2. HPGM is based on the 27-point stencil computation, and the diagonal and off-diagonal elements of the matrices are 26 and -1, respectively. The matrices from HPGMP are similar to those from HPGM; the off-diagonal values that represents the connection with forward and backward positions along the z-axis are replaced with $-1 + \beta$ and $-1 - \beta$, respectively (β was 0.5 in the experiments). It should be noted that we applied diagonal scaling to all matrices. In each test, the right-hand side was a random vector, whose elements were uniformly distributed in the range [0, 1).

We measured the average iteration counts and execution time of three runs. Starting with an initial guess of a zero vector, each solver ran to reach an approximate solution \tilde{x} that satisfies

$$\frac{\|b - A\tilde{x}\|_2}{\|b\|_2} < 1.0 \times 10^{-8}.$$

When convergence stalled, we terminated F3R after 300 outermost iterations; that is, F3R was restarted only three times. Similarly, FGMRES(64), CG, and BiCGStab were terminated after 19,200 iterations.

5.1 Experiments on a CPU Node

First, we conducted experiments on a CPU node of the Camphor 3 supercomputer at Kyoto University. A block-Jacobi ILU(0) (or IC(0) when symmetric) preconditioner was used as the primary preconditioner M for multi-threading.

Table 2: Test matrices. n_{nz} denotes the number of nonzeros. The suffix x_y_z for matrices from HPCG and HPGMP denotes the problem size in \log_2 for each of the x, y, and z axes.

Matrix	n	n_{nz}	n_{nz}/n	α_{ILU}	α_{AINV}
Bump_2911	2,911,419	127,729,899	43.87	1.1	1.2
Emilia_923	923,136	40,373,538	43.74	1.0	1.2
G3_circuit	1,585,478	7,660,826	4.83	1.0	1.0
Queen_4147	4,147,110	316,548,962	76.33	1.1	1.3
Serena	1,391,349	64,131,971	46.09	1.1	1.2
apache2	715,176	4,817,870	6.74	1.0	1.0
audikw_1	943,695	77,651,847	82.28	1.1	1.6
ecology2	999,999	4,995,991	5.00	1.0	1.0
hpcg_7_7_7	2,097,152	55,742,968	26.58	1.0	1.0
hpcg_8_7_7	4,194,304	111,777,784	26.65	1.0	1.0
hpcg_8_8_7	8,388,608	224,140,792	26.72	1.0	1.0
hpcg_8_8_8	16,777,216	449,455,096	26.79	1.0	1.0
ldoor	952,203	42,493,817	44.63	1.1	1.3
thermal2	1,228,045	8,580,313	6.99	1.0	1.0
tmt_sym	726,713	5,080,961	6.99	1.0	1.0
<hr/>					
Freescale1	3,428,755	17,052,626	4.97	1.1	1.1
Transport	1,602,111	23,487,281	14.66	1.0	1.0
atmosmodd	1,270,432	8,814,880	6.94	1.0	1.0
atmosmodj	1,270,432	8,814,880	6.94	1.0	1.0
atmosmodl	1,489,752	10,319,760	6.93	1.0	1.0
hpgmp_7_7_7	2,097,152	55,742,968	26.58	1.0	1.0
hpgmp_8_7_7	4,194,304	111,777,784	26.65	1.0	1.0
hpgmp_8_8_7	8,388,608	224,140,792	26.72	1.0	1.0
hpgmp_8_8_8	16,777,216	449,455,096	26.79	1.0	1.0
rajat31	4,690,002	20,316,253	4.33	1.0	1.0
ss	1,652,680	34,753,577	21.03	1.1	1.2
stokes	11,449,533	349,321,980	30.51	1.0	1.3
t2em	921,632	4,590,832	4.98	1.0	1.0
tmt_unsym	917,825	4,584,801	5.00	1.0	1.0
vas_stokes_1M	1,090,664	34,767,207	31.88	1.0	1.3
vas_stokes_2M	2,146,677	65,129,037	30.34	1.0	1.3

The number of blocks was 112 ($= 56 \times 2$) because the used node has two Intel Sapphire Rapids CPUs with 56 cores. Additionally, to stabilize block-Jacobi ILU(0), we used a technique that scales diagonal elements of \mathbf{A} only during the ILU factorization; specifically, the ILU factorization was applied to a matrix obtained by multiplying the diagonal elements of \mathbf{A} by a problem-dependent real number, α_{ILU} . The value of α_{ILU} was determined such that CG or BiCGStab performed better, listed in Table 2.

The coefficient matrix and preconditioner were stored in the compressed sparse row format. All vector and matrix-vector operations were multi-threaded in a row-wise manner with 112 threads. The used compiler was the Intel oneAPI DPC++/C++ Compiler (ver. 2023.2.4) with options `-std=c++17 -fast -qopenmp -xCORE-AVX512 -mavx512fp16 -qnnextgen`. We also specified `numactl --interleave=all` at runtime to suppress the variability and deterioration of execution performance.

Figure 1 shows the relative performance, with the upper plot for symmetric matrices and the lower plot for non-symmetric matrices. The tables accompanying the plots show the average execution time (in seconds) for the baseline fp64-F3R (bottom rows) and the values of m_2 , m_3 , and m_4 for fp16-F3R-best in m_2 - m_3 - m_4 (top rows). The results for apache2, Freescale1, and rajat31 are omitted because no solver converged. Table 3 shows the number of preconditioning steps required for convergence for each of fp64-FGMRES(64), fp64-CG (or fp64-BiCGStab), and the three implementations of F3R.

First, we analyze the performance balance among the three implementations of F3R: fp64-F3R, fp32-F3R, and fp16-F3R. As shown in Table 3, there is no significant difference in the convergence rate, regardless of the use of lower-precision arithmetic in F3R. Even in the cases where the number of iterations increased, such as hpgmp_8_8_8, the rate was at most 9%. Furthermore, in some cases, fp16-F3R converged in fewer iterations than fp64-F3R and fp32-F3R. These results confirm that using low-precision arithmetic in inner solvers with a limited number of iterations does not slow down convergence. This compatibility with low-precision arithmetic contributed to the speedups shown in Figure 1.

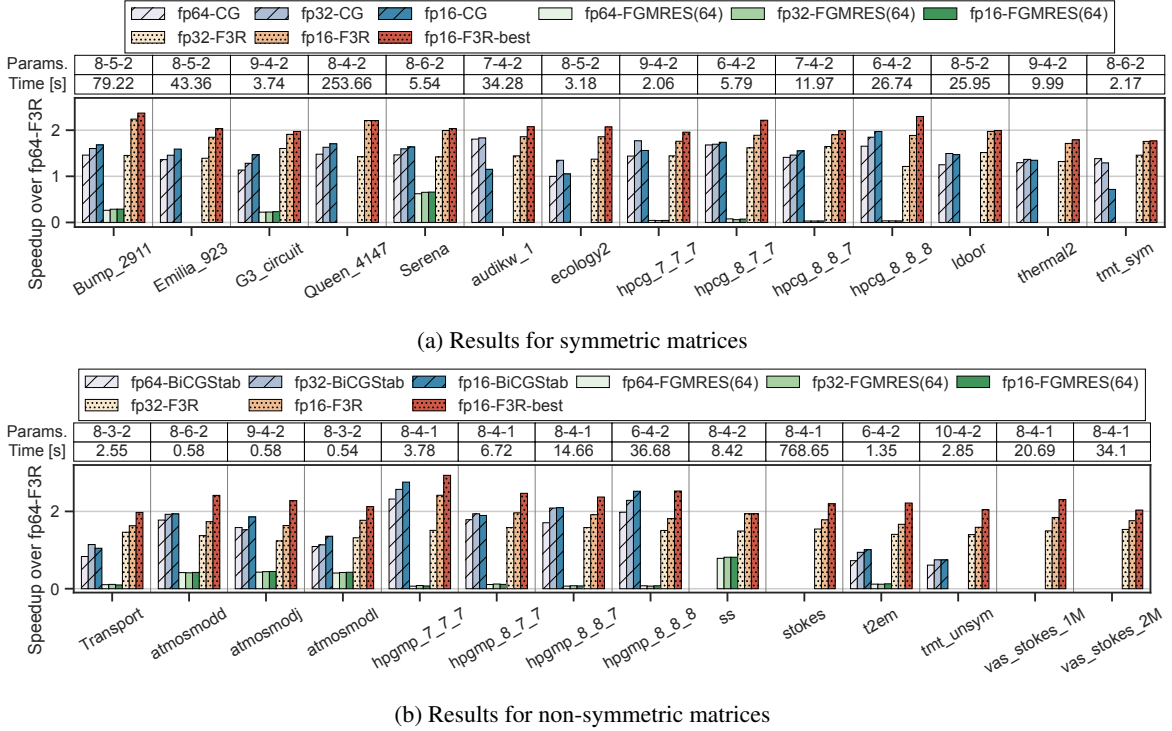


Figure 1: Performance relative to fp64-F3R on the CPU node. No bar indicates that the convergence failed. Each table above the plots shows the parameters of fp16-F3R-best in $m_2-m_3-m_4$ at the top row and the execution time of baseline, fp64-F3R, in seconds at the bottom row.

Specifically, fp32-F3R outperformed fp64-F3R across all tested problems, with an average speedup of about $1.46\times$. Furthermore, fp16-F3R surpassed fp32-F3R, achieving speedups over fp64-F3R ranging from $1.59\times$ to $2.42\times$ and over fp32-F3R from $1.11\times$ to $1.60\times$. Unlike previous methods, our approach consistently benefits from fp16 arithmetic, demonstrating the superiority of our approach.

Next, we compare F3R with other standard Krylov solvers. In terms of execution performance, F3R significantly outperformed FGMRES(64) in all tests, regardless of implementation. Notably, fp16-F3R achieved a speedup of up to $58.06\times$ over fp16-FGMRES(64), even when restricted to problems that fp16-FGMRES(64) could solve. This superiority of fp16-F3R stems from nesting FGMRES to reduce the computational cost in the Arnoldi process. These results suggest that fp16-F3R will outperform existing fp32-fp64 mixed-precision GMRES solvers because their performance is generally expected to be at most twice that of fp64 GMRES. Regarding the convergence speed in terms of the number of primary preconditioning steps, F3R also generally outperformed FGMRES(64), converging with up to 74% fewer preconditioning steps. Additionally, F3R was able to solve `tmt_unsym` and `ecology2` with relatively few iterations, whereas FGMRES(64) failed, reinforcing the idea that nesting is more effective for convergence than restarting.

Compared to CG and BiCGStab, F3R demonstrated comparable or superior performance. Specifically, fp16-F3R outperformed fp64-CG and fp64-BiCGStab in 14/14 and 12/14 cases, respectively, with speedups ranging from $1.02\times$ to $1.86\times$ for CG and $1.03\times$ to $2.60\times$ for BiCGStab. Even against fp16-CG and fp16-BiCGStab, fp16-F3R performed better in 13/14 and 9/14 cases, respectively. Table 3 further shows that the convergence speed of F3R was comparable to CG and BiCGStab, especially for problems where all solvers required a relatively large number of iterations, such as `Bump_2911` and `Transport`. On the other hand, for relatively easier problems such as `hpcg_8_8_8`, F3R tended to require noticeably more iterations than CG or BiCGStab. This may be attributed to the nested structure, which merges the results of inner solvers for segmented Krylov subspaces, rather than searching an overall Krylov subspace. However, considering that CG is the de facto standard for symmetric positive definite linear systems, the effectiveness of F3R, which does not rely on symmetry, is particularly noteworthy. Furthermore, F3R successfully converged on problems where BiCGStab failed, suggesting that F3R is more stable due to the monotonically decreasing behavior of FGMRES.

Table 3: Number of invocations of the primary preconditioner M until convergence on CPU experiments. Hyphens indicate that the convergence failed.

Matrix	CG or		fp64-	fp32-	fp16-
	BiCGStab	FGMRES(64)			
Bump_2911	4549	15833	5312	5312	5248
Emilia_923	8696	-	11136	11072	11008
G3_circuit	1570	2772	1664	1664	1728
Queen_4147	6748	-	7744	7616	7616
Serena	659	913	832	832	832
audikw_1	2820	-	3968	4032	4032
ecology2	2421	-	2880	2816	2880
hpcg_7_7_7	249	371	384	384	384
hpcg_8_7_7	350	554	512	512	512
hpcg_8_8_7	410	802	512	512	512
hpcg_8_8_8	332	829	512	512	512
ldoor	4965	-	5824	5824	5888
thermal2	3911	-	4480	4480	4544
tmt_sym	1761	-	2112	2112	2048
Transport	1060	3477	896	896	896
atmosmodd	214	274	320	320	320
atmosmodj	236	254	320	320	320
atmosmodl	264	227	256	256	256
hpgmp_7_7_7	292	416	640	640	512
hpgmp_8_7_7	368	417	576	576	576
hpgmp_8_8_7	416	436	640	640	640
hpgmp_8_8_8	388	512	704	704	768
ss	-	1246	1792	1792	1664
stokes	-	-	14976	15296	15488
t2em	1770	3056	1216	1216	1216
tmt_unsym	4374	-	2624	2624	2688
vas_stokes_1M	-	-	4416	4416	4480
vas_stokes_2M	-	-	3840	3840	3904

Finally, while fp16-F3R performed comparably to fp16-F3R-best for some problems, fp16-F3R-best achieved the highest performance across all tests. It was faster than fp16-CG, fp16-BiCGStab, and fp16-FGMRES(64) by up to $2.47\times$, $2.74\times$, and $69.10\times$, respectively. These results indicate the promise of optimizing the parameters and suggests that F3R has potential for improvement. This aspect will be explored in Section 6.1 with additional experiments.

5.2 Experiments on a GPU Node

Next, we present results obtained on a GPU node of the Gardenia supercomputer at Kyoto University. The node has four NVIDIA A100 GPUs, but the experiments used a single GPU. We employed the SD-AINV preconditioner (Suzuki et al., 2022), a simplified version of the standard approximate inverse preconditioner (Benzi et al., 1996), for M to exploit the GPU parallelism. SD-AINV requires only two sparse matrix-vector multiplications (SpMVs) per preconditioning step and is well-suited for GPU implementation. As with block-Jacobi ILU(0), we scaled the diagonal elements of A by a real number α_{AINV} during the preconditioner construction. The value of α_{AINV} is listed in Table 2.

All GPU kernels were implemented in CUDA to execute all computations on the GPU, except for convergence checking. The NVIDIA HPC Compiler (ver. 23.9), nvc++, was used, with the main options `-std=c++17 -O3 -cuda`. Unlike the CPU experiments, the SpMV kernels were implemented using the sliced ELLPACK format (Monakov et al., 2010) with a chunk size of 32.

The GPU experiments showed results similar to those of the CPU experiments. As shown in Figure 2, fp32-F3R outperformed fp64-F3R, while fp16-F3R was even faster than fp32-F3R. Moreover, all three implementations of F3R exhibited similar convergence speeds for most problems, indicating that F3R can effectively incorporate fp16 arithmetic. While F3R with the default setting performed well, fp16-F3R-best achieved even better results, suggesting room for optimization. F3R generally converged faster than FGMRES(64) and performed comparably to CG and BiCGStab. Specifically, it was faster than FGMRES(64) in all the tests except for `rajat31`, achieving speedups ranging from $2.16\times$ to $28.18\times$. Additionally, F3R outperformed CG and BiCGStab in many cases; fp16-F3R performed better

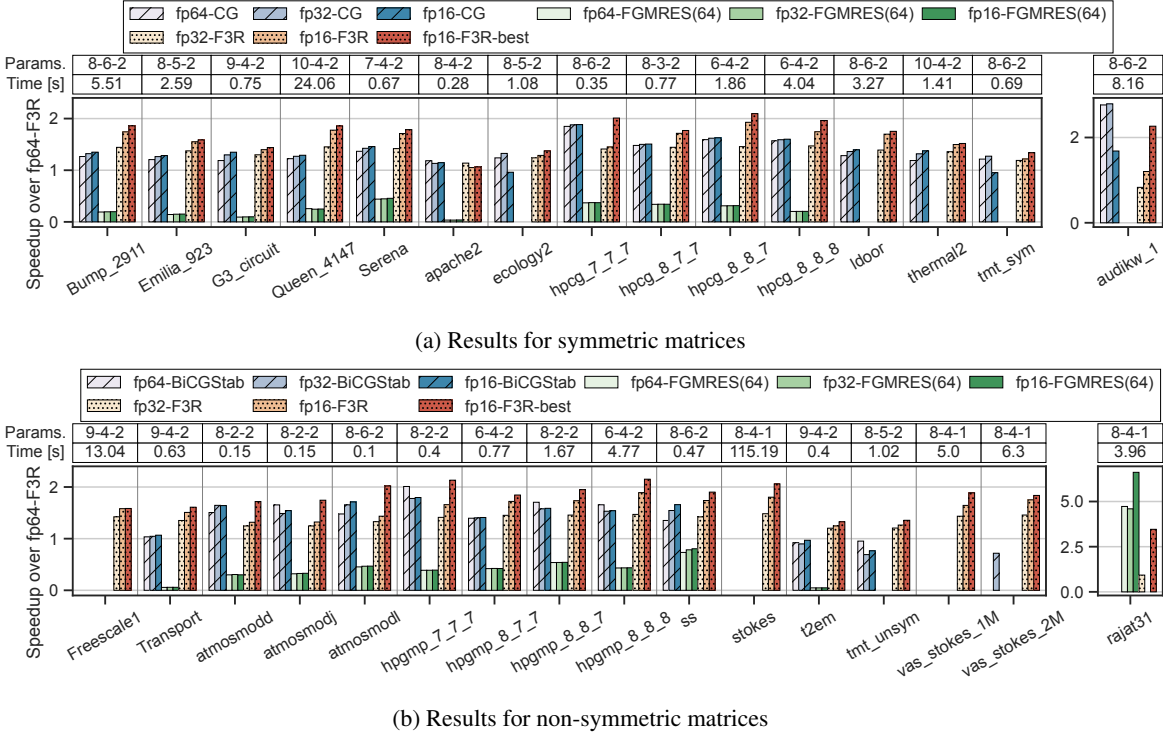


Figure 2: Performance relative to fp64-F3R on the GPU node. No bar indicates that the convergence failed. Each table above the plots shows the parameters of fp16-F3R-best in m_2 - m_3 - m_4 at the top row and the execution time of baseline, fp64-F3R, in seconds at the bottom row.

than fp16-CG in 11 out of 15 cases and fp16-BiCGStab in 11 out of 16 cases. These results confirm that F3R is also well-suited for GPU implementation and can be effectively combined with the approximate inverse-type preconditioner.

However, two main differences should be noted. First, in the case of `rajat31`, F3R underperformed FGMRES(64), suggesting the existence of a class of problems where nesting FGMRES may degrades the convergence speed; that is, Assumption (i) does not hold. Second, the speedup achieved by reducing precision to fp32 and fp16 was moderate, $1.34\times$ and $1.55\times$ on average, compared to $1.46\times$ and $1.87\times$ in the CPU experiments. This could be attributed to using a different preconditioner and differences in memory bandwidth and cache utilization between CPUs and GPUs. F3R requires storing matrix values in fp64, fp32, and fp16, which incurs an overhead and may not have been suitable for the GPU. To further improve the performance on GPUs, developing a framework that enhances cache efficiency would be necessary.

6 Experiments on Parameter Setting

In Section 5, we have focused on the results with the default parameters, $(m_1, m_2, m_3, m_4) = (100, 8, 4, 2)$ and $c = 64$, and demonstrated that these are relatively good but also has room for optimization. Thus, in this section, we investigate different settings of these parameters with additional experiments on the CPU node. Furthermore, we discuss the propriety of four-level nesting and using the Richardson iteration in the innermost solver, namely Assumptions (i) and (ii).

6.1 On the Number of Inner Iterations

First, we examine the number of iterations of each inner solver, m_2 , m_3 , and m_4 . Figure 3 illustrates trends in the performance of fp16-F3R when varying the values of m_2 , m_3 , and m_4 , showing the relationships between execution performance and convergence speed relative to the default setting. Values > 1 on both axes indicate better performance than fp16-F3R. We begin by analyzing the effect of m_4 , the number of the innermost Richardson iterations. The results for $m_4 = 3$ and $m_4 = 4$ show that increasing m_4 generally reduced the convergence speed rather than improving it.

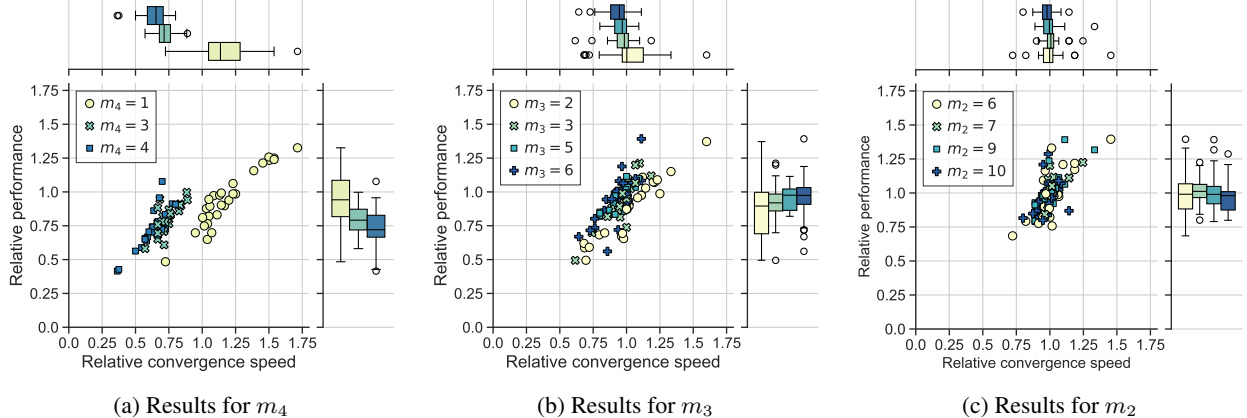


Figure 3: Results for different values of m_2 , m_3 , and m_4 . Boxplots on the right and top correspond to the y- and x-axis respectively. The results are relative to fp16-F3R with the default setting ($m_2, m_3, m_4 = 8, 4, 2$), and the larger, the better in both axes.

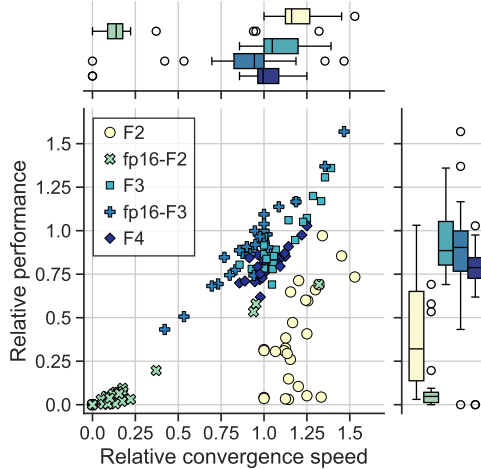


Figure 4: Relationship between performance and the depth of nesting. The results are relative to fp16-F3R with the default setting, and the larger, the better.

This degradation directly led to poor execution performance because the innermost Richardson accounts for a certain amount of computation in fp16-F3R. This result suggests that Assumption (ii) does not hold for $m = 3, 4$. In contrast, the setting of $m_4 = 1$ demonstrated better convergence speeds for several problems, though its execution performance was generally lower than that of $m_4 = 2$. In the case of $m_4 = 1$, the Richardson part, (R_{m_4}, M) , is equivalent to the standard preconditioner, M , if the weight is not taken into account, meaning all iterations are performed by FGMRES. This explains why $m_4 = 2$ often outperforms $m_4 = 1$: a single Richardson iteration involves considerably fewer computations than an FGMRES iteration.

Next, we inspect the effects of m_3 and m_2 . Compared to m_4 , both had a smaller effect; that is, no clear relationship was observed between them and the performance of fp16-F3R. Increasing m_3 slightly improved the convergence rate; however, since it also increased the computational cost per outermost iteration, the overall execution performance remained relatively unchanged. Notably, depending on the problem, the performance fluctuated within a range of approximately 50–140% when comparing $m_3 = 2$ and $m_3 = 6$ against the default value $m_3 = 4$. This suggests that m_3 , in particular, offers room for optimization, e.g., through adaptive methods. Similarly, the effect of m_2 was small, especially in terms of the variance of the convergence speed; the change was less than 10% in most tested problems. The execution performance varied slightly more because of changes in computational cost per outermost iteration, but its effect was still minor compared to m_4 and m_3 .

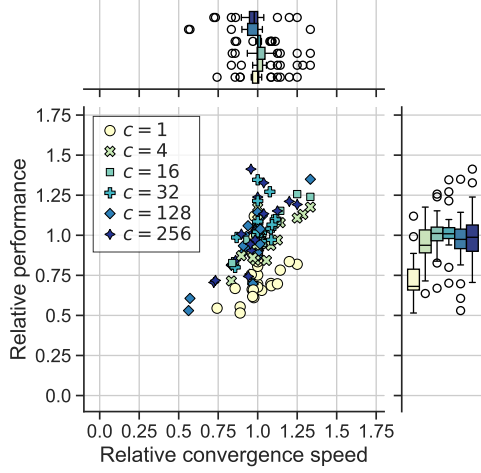


Figure 5: Performance balance when changing the weight-updating cycle c in the Richardson part. The results are relative to fp16-F3R with $c = 64$.

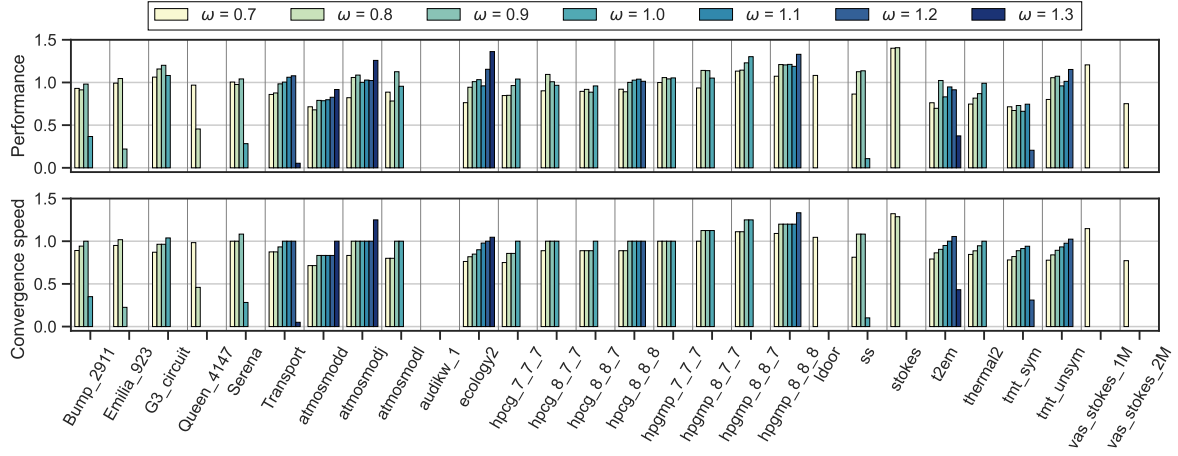


Figure 6: fp16-F3R with the adaptive strategy vs. fp16-F3R with a fixed weight. No bar indicates that the convergence failed. The values are relative to fp16-F3R with the adaptive strategy. Values < 1 indicate that the adaptive strategy was better.

Consequently, while the default choice $m_4 = 2$ is reasonable, finding optimal values of m_2 and m_3 is more challenging as they depend strongly on the problem. In particular, m_3 has a comparatively large effect, which implies the importance of techniques to adaptively control it for further improved performance of F3R.

6.2 On the Nesting Depth

Next, we investigate the depth of nesting by showing results for five additional solvers in Figure 4. The characteristics of these solvers are summarized in Table 4. Briefly, F2 and F3 are two- and three-level nested FGMRES, respectively. Each maintains the same precision as fp16-F3R at corresponding depth levels. fp16-F2 and fp16-F3 are modified versions of F2 and F3, respectively, where the innermost solver is implemented in fp16. F4 is largely the same as fp16-F3R but replaces the innermost Richardson part with FMGRES.

Before considering the depth of nesting, we compare fp16-F3R and F4 to verify Assumption (ii). The figure shows that the convergence rates of F4 and fp16-F3R were similar, with a relatively small quartile deviation (all plots are close to 1.0), thereby validating Assumption (ii) with $m_4 = 2$. Furthermore, despite the similar convergence speed, fp16-F3R outperformed F4 for all problems except for t2em. This demonstrates that using Richardson is advantageous in terms of computational cost because it skips the Arnoldi process.

Table 4: Additional solvers used in Section 6.2

Solver	Tuple notation	Parts	Precision		
			\mathbf{A}	Vectors	\mathbf{M}
F2	(F_{100}, F_{64}, M)	F_{100}	fp64	fp64	-
		F_{64}	fp32	fp32	fp16
fp16-F2	(F_{100}, F_{64}, M)	F_{100}	fp64	fp64	-
		F_{64}	fp16	fp16	fp16
F3	(F_{100}, F_8, F_8, M)	F_{100}	fp64	fp64	-
		F_8 (outer)	fp32	fp32	-
		F_8 (inner)	fp16	fp32	fp16
fp16-F3	(F_{100}, F_8, F_8, M)	F_{100}	fp64	fp64	-
		F_8 (outer)	fp32	fp32	-
		F_8 (inner)	fp16	fp16	fp16
F4	$(F_{100}, F_8, F_4, F_2, M)$	F_{100}	fp64	fp64	-
		F_8	fp32	fp32	-
		F_4	fp16	fp32	-
		F_2	fp16	fp16	fp16

Next, we examine F2 and fp16-F2 which can be regarded as fp64-fp32 and fp64-fp16 inner-outer FGMRES, respectively. F2 was generally better than fp16-F3R in the convergence speed, but the improvement was limited, falling below 1.25 times in about 75% of the test cases. This suggests that Assumption (i) is not entirely implausible; we can replace FGMRES with a nested one without significantly degrading the convergence. In execution performance, F2 underperformed fp16-F3R because of its higher computational cost in the Arnoldi process, as mentioned in Section 4.1, indicating that nesting FGMRES has certain merit. Moreover, fp16-F2 significantly reduced the convergence speed and, in turn, execution performance. This reaffirms that using fp16 for all parts of inner (flexible) GMRES with long iterations causes a precision overflow.

Finally, we evaluate the three-level nested solvers, F3 and fp16-F3. To the best of our knowledge, three-level nested FGMRES with fp32 and fp16 has not been previously reported. For more than half of the tested problems, the proposed solver, fp16-F3R, outperformed both F3 and fp16-F3 in execution performance, underscoring the effectiveness of fp16-F3R. Moreover, the results also offer two key observations. First, F3 and F4 had similar convergence speeds for many problems. This indicates that approximating $(\mathbf{F}_8, \mathbf{M})$ with $(\mathbf{F}_4, \mathbf{F}_2, \mathbf{M})$ did not significantly degrade convergence, supporting the validity of Assumption (i). However, for several problems, such as `stokes` and `vas_stokes_2M`, F3 converged faster, resulting in better execution performance even compared to fp16-F3R. These problems are considered relatively difficult, as neither BiCGStab nor FGMRES(64) could solve them. This implies that, for difficult problems, searching a large subspace is more effective than combining results from small subspaces via the nested Krylov approach. In these cases, Assumption (i) does not hold, and we must carefully consider the number of inner iterations for better performance. Second, fp16-F3 showed slower convergence than F3, indicating that eight iterations are still excessive to perform FGMRES in fp16 without exceeding precision limits. Therefore, limiting the number of fp16 iterations appears to be a practical strategy, and four-level nesting in fp16-F3R is a reasonable choice to balance convergence, execution performance, and the effective use of fp16.

6.3 On the Weight in Richardson

Finally, we discuss the weight in the Richardson part. Figure 5 compares six different values of the updating cycle, c , in the adaptive weight-updating technique. No clear trend emerges compared to the other factors discussed above, except for the case of $c = 1$. In this case, the convergence speed was not improved significantly, despite many additional computations imposed on F3R. As a result, the default setting $c = 64$ performed similar to the case of $c = 1$ for most cases. For other settings, performance varied depending on the problem. Looking more closely, a slight decrease in convergence is observed as c increases; however, execution performance does not necessarily degrade because of the fewer additional computations due to the large c .

Figure 6 compares our adaptive approach with a static one, where the weight is manually set. In some cases, such as $\omega = 1.3$ for `ecology2`, the static approach performed better. However, the adaptive approach was one of the best in most cases. Importantly, the performance of the static approach is highly sensitive to the setting. For instance, the static

approach failed on `audikw_1` for all weight values, whereas the dynamic approach succeeded. This stability against the parameter makes our adaptive technique a viable and effective option.

6.4 Summary

In this section, we have analyzed F3R from three perspectives: the number of inner iterations, the nesting depth, and the weight in Richardson. Experimental results confirmed the validity of both Assumptions (ii) and (i) within the context of our approach. However, Assumption (i) occasionally did not hold, particularly for relatively difficult problems. Additionally, the results showed that the default parameters $(m_1, m_2, m_3, m_4) = (100, 8, 4, 2)$ effectively balanced performance, convergence, and the use of fp16. Notably, the value of m_3 had a large effect on the performance of F3R, though its optimal value varied depending on problem. Since identifying it is challenging, adaptive approaches, such as dynamically controlling it based on the magnitude of the residuals, would be beneficial. Finally, it was confirmed that the adaptive weight-updating technique in Algorithm 1 provided greater stability to the parameter than using a single, fixed weight.

7 Conclusions

We proposed a solver, F3R, based on a novel mixed-precision approach that integrates FGMRES and Richardson solvers in the nested Krylov structure. Numerical experiments confirmed that this approach is suited for using fp16 arithmetic without increasing the total number of iterations. Additionally, the results showed that F3R is more stable than BiCGStab and achieves comparable or superior performance to CG, BiCGstab, and restarted FGMRES. This is because F3R requires relatively fewer computations in the Arnoldi process compared to restarted FGMRES. Experiments presented in Section 6 indicated that the parameters used in Section 5 are reasonable, though there is still potential for improvement, especially in the number of iterations performed by the middle solvers.

Future direction includes the following three. The first is conducting more comprehensive evaluations. Since F3R relies solely on FGMRES and Richardson, it can apply asynchronous preconditioners, which could also be advantageous. Moreover, other Krylov methods also accept various approaches to reducing precision beyond simply using lower-precision preconditioners, although these would need parameter optimization. These methods may change the performance balance. The second direction is introducing dynamic techniques for terminating inner iterations. For instance, a strategy based on magnitude of inner residuals could be beneficial. The third direction is extending F3R for distributed systems. Notably, the innermost Richardson part does not incorporate a reduction process, which typically involves collective communication. Furthermore, the inner FGMRES solvers perform only a limited number of iterations per parent iteration, making them well-suited for communication-avoiding implementations (Hoemmen, 2010; Yamazaki et al., 2024).

Acknowledgement

This work was supported by JSPS KAKENHI Grant Number JP24KJ0266.

References

Ahmad Abdelfattah, Hartwig Anzt, Erik G Boman, Erin Carson, Terry Cojean, Jack Dongarra, Alyson Fox, Mark Gates, Nicholas J Higham, Xiaoye S Li, et al. 2021. A survey of numerical linear algebra methods utilizing mixed-precision arithmetic. *The International Journal of High Performance Computing Applications* 35, 4 (2021), 344–369. doi:10.1177/10943420211003313

Ahmad Abdelfattah, Stan Tomov, and Jack Dongarra. 2020. Investigating the Benefit of FP16-Enabled Mixed-Precision Solvers for Symmetric Positive Definite Matrices Using GPUs. In *International Conference on Computational Science*. Springer, Springer International Publishing, Cham, 237–250. doi:10.1007/978-3-030-50417-5_18

José I Aliaga, Hartwig Anzt, Thomas Grützmacher, Enrique S Quintana-Ortí, and Andrés E Tomás. 2023. Compressed basis GMRES on high-performance graphics processing units. *The International Journal of High Performance Computing Applications* 37, 2 (2023), 82–100. doi:10.1177/10943420221115140

Patrick Amestoy, Alfredo Buttari, Nicholas J Higham, Jean-Yves L'Excellent, Théo Mary, and Bastien Vieublé. 2024. Five-Precision GMRES-Based Iterative Refinement. *SIAM J. Matrix Anal. Appl.* 45, 1 (2024), 529–552. doi:10.1137/23M1549079

Hartwig Anzt, Vincent Heuveline, and Björn Rocker. 2011. An Error Correction Solver for Linear Systems: Evaluation of Mixed Precision Implementations. In *High Performance Computing for Computational Science—VECPAR 2010*:

9th International conference, Berkeley, CA, USA, June 22-25, 2010, Revised Selected Papers 9. Springer, 58–70. doi:10.1007/978-3-642-19328-6_8

Owe Axelsson, Zhong-Zhi Bai, and Shou-Xia Qiu. 2004. A Class of Nested Iteration Schemes for Linear Systems with a Coefficient Matrix with a Dominant Positive Definite Symmetric Part. *Numerical Algorithms* 35 (2004), 351–372. doi:10.1023/B:NUMA.0000021766.70028.66

Marc Baboulin, Alfredo Buttari, Jack Dongarra, Jakub Kurzak, Julie Langou, Julien Langou, Piotr Luszczek, and Stanimire Tomov. 2009. Accelerating scientific computations with mixed precision algorithms. *Computer Physics Communications* 180, 12 (2009), 2526–2533. doi:10.1016/j.cpc.2008.11.005

Michele Benzi, Carl D Meyer, and Miroslav Tůma. 1996. A Sparse Approximate Inverse Preconditioner for the Conjugate Gradient Method. *SIAM Journal on Scientific Computing* 17, 5 (1996), 1135–1149. doi:10.1137/S1064827594271421

Alfredo Buttari, Jack Dongarra, Jakub Kurzak, Piotr Luszczek, and Stanimir Tomov. 2008. Using Mixed Precision for Sparse Matrix Computations to Enhance the Performance while Achieving 64-bit Accuracy. *ACM Transactions on Mathematical Software (TOMS)* 34, 4 (2008), 1–22. doi:10.1145/1377596.1377597

Erin Carson, Tomáš Gergelits, and Ichitaro Yamazaki. 2022. Mixed precision s-step Lanczos and conjugate gradient algorithms. *Numerical Linear Algebra with Applications* 29, 3 (2022), e2425. doi:10.1002/nla.2425

Erin Carson and Nicholas J Higham. 2017. A New Analysis of Iterative Refinement and Its Application to Accurate Solution of Ill-Conditioned Sparse Linear Systems. *SIAM Journal on Scientific Computing* 39, 6 (2017), A2834–A2856. doi:10.1137/17M1122918

Erin Carson and Noaman Khan. 2023. Mixed Precision Iterative Refinement with Sparse Approximate Inverse Preconditioning. *SIAM Journal on Scientific Computing* 45, 3 (2023), C131–C153. doi:10.1137/22M1487709

Timothy A Davis and Yifan Hu. 2011. The University of Florida sparse matrix collection. *ACM Transactions on Mathematical Software (TOMS)* 38, 1 (2011), 1–25. doi:10.1145/2049662.2049663

Jack Dongarra, Michael A Heroux, and Piotr Luszczek. 2016. A new metric for ranking high-performance computing systems. *National Science Review* 3, 1 (2016), 30–35. doi:10.1093/nsr/nwv084

Gene H Golub and Qiang Ye. 1999. Inexact Preconditioned Conjugate Gradient Method with Inner-Outer Iteration. *SIAM Journal on Scientific Computing* 21, 4 (1999), 1305–1320. doi:10.1137/S1064827597323415

Stef Graillat, Fabienne Jézéquel, Théo Mary, and Roméo Molina. 2024. Adaptive Precision Sparse Matrix–Vector Product and Its Application to Krylov Solvers. *SIAM Journal on Scientific Computing* 46, 1 (2024), C30–C56. doi:10.1137/22M1522619

Thomas Grützmacher, Robert Underwood, Sheng Di, Franck Cappello, and Hartwig Anzt. 2024. FRSZ2 for In-Register Block Compression Inside GMRES on GPUs. In *SC24-W: Workshops of the International Conference for High Performance Computing, Networking, Storage and Analysis*. 240–249. doi:10.1109/SCW63240.2024.00038

Azzam Haidar, Stanimire Tomov, Jack Dongarra, and Nicholas J Higham. 2018. Harnessing GPU Tensor Cores for Fast FP16 Arithmetic to Speed up Mixed-Precision Iterative Refinement Solvers. In *SC18: International Conference for High Performance Computing, Networking, Storage and Analysis*. IEEE, 603–613. doi:10.1109/SC.2018.00050

Nicholas J Higham and Theo Mary. 2022. Mixed precision algorithms in numerical linear algebra. *Acta Numerica* 31 (2022), 347–414. doi:10.1017/S0962492922000022

Nicholas J Higham and Srikara Pranesh. 2021. Exploiting Lower Precision Arithmetic in Solving Symmetric Positive Definite Linear Systems and Least Squares Problems. *SIAM Journal on Scientific Computing* 43, 1 (2021), A258–A277. doi:10.1137/19M1298263

Mark Hoemmen. 2010. *Communication-avoiding Krylov subspace methods*. University of California, Berkeley.

Neil Lindquist, Piotr Luszczek, and Jack Dongarra. 2021. Accelerating Restarted GMRES With Mixed Precision Arithmetic. *IEEE Transactions on Parallel and Distributed Systems* 33, 4 (2021), 1027–1037. doi:10.1109/TPDS.2021.3090757

Jennifer A Loe, Christian A Glusa, Ichitaro Yamazaki, Erik G Boman, and Sivasankaran Rajamanickam. 2021. Experimental Evaluation of Multiprecision Strategies for GMRES on GPUs. In *2021 IEEE International Parallel and Distributed Processing Symposium Workshops (IPDPSW)*. IEEE, 469–478. doi:10.1109/IPDPSW52791.2021.00078

Lois Curfman McInnes, Barry Smith, Hong Zhang, and Richard Tran Mills. 2014. Hierarchical Krylov and nested Krylov methods for extreme-scale computing. *Parallel Comput.* 40, 1 (2014), 17–31. doi:10.1016/j.parco.2013.10.001

Alexander Monakov, Anton Lokhmotov, and Arutyun Avetisyan. 2010. Automatically Tuning Sparse Matrix-Vector Multiplication for GPU Architectures. In *High Performance Embedded Architectures and Compilers: 5th International Conference, HiPEAC 2010, Pisa, Italy, January 25-27, 2010. Proceedings 5*. Springer, 111–125. doi:10.1007/978-3-642-11515-8_10

Lewis Fry Richardson. 1911. IX. The approximate arithmetical solution by finite differences of physical problems involving differential equations, with an application to the stresses in a masonry dam. *Philosophical Transactions of the Royal Society of London. Series A, Containing Papers of a Mathematical or Physical Character* 210, 459-470 (1911), 307–357. doi:10.1098/rsta.1911.0009

Youcef Saad. 1993. A Flexible Inner-Outer Preconditioned GMRES Algorithm. *SIAM Journal on Scientific Computing* 14, 2 (1993), 461–469. doi:10.1137/0914028

Yousef Saad. 2003. *Iterative methods for sparse linear systems*. SIAM.

Jennifer Scott and Miroslav Tůma. 2024. Avoiding Breakdown in Incomplete Factorizations in Low Precision Arithmetic. *ACM Trans. Math. Software* 50, 2 (2024), 1–25. doi:10.1145/3651155

Valeria Simoncini and Daniel B Szyld. 2003. Theory of Inexact Krylov Subspace Methods and Applications to Scientific Computing. *SIAM Journal on Scientific Computing* 25, 2 (2003), 454–477. doi:10.1137/S1064827502406415

Kengo Suzuki, Takeshi Fukaya, and Takeshi Iwashita. 2022. A New AINV Preconditioner for the CG Method in Hybrid CPU-GPU Computing Environment. *Journal of Information Processing* 30 (2022), 755–765. doi:10.2197/ipsjjip.30.755

Kengo Suzuki, Takeshi Fukaya, and Takeshi Iwashita. 2024. An Integer Arithmetic-Based AMG Preconditioned FGMRES Solver. *ACM Trans. Math. Software* (2024). doi:10.1145/3704726

Kathryn Turner and Homer F Walker. 1992. Efficient High Accuracy Solutions with GMRES(m). *SIAM journal on scientific and statistical computing* 13, 3 (1992), 815–825. doi:10.1137/0913048

Ichitaro Yamazaki, Christian Glusa, Jennifer Loe, Piotr Luszczek, Sivasankaran Rajamanickam, and Jack Dongarra. 2022. High-Performance GMRES Multi-Precision Benchmark: Design, Performance, and Challenges. In *2022 IEEE/ACM International Workshop on Performance Modeling, Benchmarking and Simulation of High Performance Computer Systems (PMBS)*. IEEE, 112–122. doi:10.1109/PMBS56514.2022.00015

Ichitaro Yamazaki, Andrew J Higgins, Erik G Boman, and Daniel B Szyld. 2024. Two-Stage Block Orthogonalization to Improve Performance of s-step GMRES. In *2024 IEEE International Parallel and Distributed Processing Symposium (IPDPS)*. IEEE, 26–37. doi:10.1109/IPDPS57955.2024.00012

Yingqi Zhao, Takeshi Fukaya, and Takeshi Iwashita. 2023. Numerical Behavior of Mixed Precision Iterative Refinement Using the BiCGSTAB Method. *Journal of Information Processing* 31 (2023), 860–874. doi:10.2197/ipsjjip.31.860

Yingqi Zhao, Takeshi Fukaya, Linjie Zhang, and Takeshi Iwashita. 2022. Numerical Investigation into the Mixed Precision GMRES(m) Method Using FP64 and FP32. *Journal of Information Processing* 30 (2022), 525–537. doi:10.2197/ipsjjip.30.525

Yi Zong, Peinan Yu, Haopeng Huang, and Wei Xue. 2024. FP16 Acceleration in Structured Multigrid Preconditioner for Real-World Applications. In *Proceedings of the 53rd International Conference on Parallel Processing*. 52–62. doi:10.1145/3673038.3673040